Journal of Computational Physics 227 (2008) 10078–10093

Contents lists available at ScienceDirect

Journal of Computational Physics

journal homepage: www.elsevier.com/locate/jcp

# Variational boundary conditions for molecular dynamics simulations: Treatment of the loading condition ☆

Xiantao Li *

*Department of Mathematics, Pennsylvania State University, University Park, PA 16802, United States*

ARTICLE INFO

*Article history:*
Received 11 January 2008
Received in revised form 4 August 2008
Accepted 9 August 2008
Available online 27 August 2008

*PACS:*
31.15.Qg
83.10.Mj
61.43.Bn

ABSTRACT

This paper aims to extend the variational boundary conditions for molecular dynamics simulation [X. Li, W. E, Variational boundary conditions for molecular dynamics simulations of solids at low temperature, Commun. Comp. Phys. 1 (2006) 136–176; X. Li, W. E, Boundary conditions for molecular dynamics simulations at finite temperature: treatment of the heat bath, Phys. Rev. B 76 (2007) 104107], to take into account external loading conditions. Two derivations of the exact boundary conditions are presented, one with Mori–Zwanzig projection procedure, and the other using lattice Green's functions. Approximate boundary conditions, which are more efficient in practice, are then discussed. Finally several numerical experiments are presented to demonstrate the effectiveness of these methods.



## 1. Introduction

The main purpose of this paper is to present a systematic approach for finding proper boundary conditions for molecular dynamics in solids. Due to the computational complexity, such simulations are typically done on rather small systems truncated from a much larger sample. As a result, artificial boundaries are introduced, where boundary conditions are needed to take into account the effect of the atoms that have been removed. Ideally, these boundary conditions should guarantee that the system behaves in the same way as if the whole sample is being simulated. In particular, the boundary conditions should play the following roles:

1. eliminate phonon reflections at the boundary,
2. introduce phonon from the surrounding heat bath to model thermal effect,
3. maintain remote loading.

Some of these issues have been addressed before. For example, several non-reflecting boundary conditions have been proposed [6,14,13,26,19,39,40] to prevent the boundary reflection and minimize the interference with the numerical results. Boundary conditions modeling heat bath are suggested in [22,27]. However, boundary conditions that account for external loading, which is needed to study various properties of material response, have not been extensively studied.

In many material simulations, it is essential to understand how defects initiate and propagate under different external loading condition in order to understand the micromechanical processes. One approach to model external loading is to

☆ Research supported by NSF Grant DMS-0609610.
* Tel.: +1 814 8639081.
*E-mail address:* xli@math.psu.edu

0021-9991/$ - see front matter © 2008 Elsevier Inc. All rights reserved.
doi:10.1016/j.jcp.2008.08.010

use the classical molecular dynamics methods for NPT ensemble [3,17,18,21,29,30,34]. These techniques aim to bring the system to an isothermal/isobaric equilibrium, thereby maintaining the system at a constant temperature/pressure state. Typically in these methods, auxiliary variables are introduced to mimic the interaction with a heat/pressure bath. In addition periodic boundary conditions are usually used. While these methods have been quite useful in predicting constitutive equations and studying phase transitions, they might misrepresent the true dynamics of the system, such as phonon emission and defect propagations.

Another approach to apply loading condition is to directly control the displacement of the atoms at the boundary, or apply additional forces, e.g. see [7,20,28]. These methods are similar to experimental techniques, such as dead loading and applying traction. However, since the system being simulated is usually much smaller than the real sample, with these methods the computational results would be inevitably subject to boundary effect.

To find the physically correct boundary condition, we start with a sample of realistic size, from which our computational domain is selected. The surround region acts as the pressure/heat bath. We then use a dimension reduction technique to eliminate the degrees of freedom associated with the atoms in the bath. As a result, the correct boundary condition is derived, which only involves the preselected atoms.

The resulting equations (see Eq. (26)) are known as the generalized Langevin equations. A key quantity there is the memory term, which comes from the coarse-graining procedure. Although in principle exact solutions can be found for the memory kernels, they are quite *non-local*: They involve many atoms and their previous history. Therefore they are very difficult to implement in practice. To find approximate kernels that are practical, we use the variational formulation [26,41,27], which finds *local* boundary conditions with optimal accuracy. Meanwhile the external loading will appear in the generalized Langevin equation as an external force. We will discuss how the external force can be computed.

This rest of this paper is organized as follows. In Section 2, we derive the exact boundary condition using a dimension reduction technique. We also present an alternative derivation using lattice Green's functions. We then discuss the implementation in actual molecular dynamics simulation. Finally, in Section 5, we show several numerical experiments to demonstrate these methods.

## 2. Derivation of the boundary condition

In this section, we will derive boundary conditions in the presence of a heat/pressure bath. We have in mind a sample of realistic size, $\Omega$, from which our computational domain, denoted by $\mathcal{D}$, will be selected. The rest of the system, denoted by $\mathcal{B}$, will act as a heat/pressure reservoir. This decomposition is shown in Fig. 1.

In this paper, the interface between the computational domain and the bath region will be referred to as the boundary, created by removing the surrounding atoms, while the physical boundary will be called the *remote boundary* since in practice the bath region is far larger than the computational domain. Typically the computational domain contains the defects under study, and loading condition needs to be applied to allow the defects to develop. This can be done by (1) applying loading conditions at the remote boundary; (2) preparing the bath region according to certain elastic field. The latter method has been widely used in MD simulations, using existing analytical solutions. Examples include the solution for an elliptical crack by Sih and Liebowitz [36] and the Stroh's solution for a dislocation [37]. The purpose of this paper is to derive the boundary condition that incorporates the loading conditions.

The boundary condition will be found by eliminating the atoms in the bath while keeping the atoms in the computational domain. For this purpose we will employ the compact procedure proposed by Mori and Zwanzig [42,43,32]. To begin with, we consider a molecular dynamics system with interatomic potential $V(\mathbf{u}_1, \mathbf{u}_2, \ldots)$. The Newton's equations of motion read,

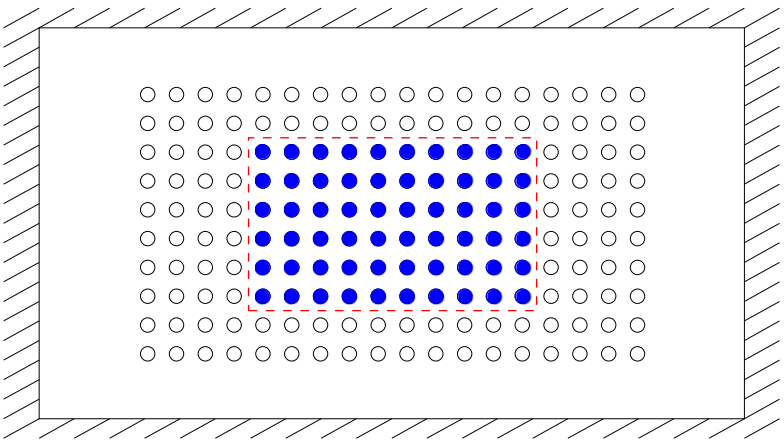

**Fig. 1.** A schematic of the boundary in 2D: filled circles represent the atoms in the computational domain; open circles are the surrounding atoms.

$$m\ddot{\mathbf{u}}_i = -\nabla_{\mathbf{u}_i} V + \mathbf{f}_i^{\mathrm{b}} \tag{1}$$

with loading force $\mathbf{f}_i^{\mathrm{b}}$ applied at the remote boundary. Here $m$ is the mass of an atom and $\mathbf{u}_i$ is the displacement. Throughout this paper, we will assume that the system has an underlying lattice structure with the equilibrium position of an atom denoted by $\mathbf{z}_i$. The displacement is the deviation of the current position, $\mathbf{r}_i$, from the reference position, i.e. $\mathbf{u}_i = \mathbf{r}_i - \mathbf{z}_i$.

In accordance with the decomposition of the domain, we divide the system into two groups: the atoms that will be included in the computation, called *retained atoms*, and the atoms in the surrounding area, called *bath atoms*. We will partition the displacement,

$$\mathbf{u} = (\mathbf{u}_I, \mathbf{u}_J), \tag{2}$$

where $\mathbf{u}_I$ and $\mathbf{u}_J$ represent the displacement of the retained atoms and bath atoms, respectively. The dimension of the system is given by $\dim(\mathbf{u}) = N$, $\dim(\mathbf{u}_I) = n$ and $\dim(\mathbf{u}_J) = N - n$. In most practical situations, $n \ll N$. We also decompose the velocity accordingly,

$$\mathbf{v} = (\mathbf{v}_I, \mathbf{v}_J). \tag{3}$$

Although the original Mori–Zwanzig formalism [5,32,42] can in principle eliminate the bath variables, the resulting equations are typically difficult to solve. Therefore we make the following approximation for the atomic interaction to simplify the results. More specifically, we linearize the interaction involving atoms in the bath, while the non-linear atomic interaction in the computational domain is retained. The new atomic potential also satisfies the following conditions:

(1) At the equilibrium state, the force on each atom should be zero.
(2) The new potential energy has the same phonon spectrum as the original potential model.

The purpose of such approximation is to keep the original atomic interaction in critical areas where local defects are present, and simplify the atomic forces away from defects where the displacement field is smooth. In the appendix, an example of this approximation is given for the embedded atom potential [12], a commonly used model for metallic materials. The linearization of the atomic potential, known as harmonic approximation [4], offers reasonable accuracy below half of the melting temperature. In practice, this approximation can be obtained by a Taylor expansion of the potential energy for the bath atoms while fixing the retained ones. The procedure leads to the total Hamiltonian in the form of,

$$\mathcal{H}(\mathbf{u}, \mathbf{v}) = \Phi(\mathbf{u}_I) + \frac{1}{2}\mathbf{u}^{\mathrm{T}} K \mathbf{u} - \mathbf{u} \cdot \mathbf{f}^{\mathrm{b}} + \frac{m}{2}\mathbf{v}^2. \tag{4}$$

Here $\Phi(\mathbf{u}_I)$ denotes the potential energy associated with the retained atoms. The matrix $K \in \mathbb{R}^{N\times N}$ consists of the force constant computed from the interatomic potential,

$$K_{ij} = \nabla^2_{\mathbf{u}_i,\mathbf{u}_j} V,$$

at the reference state. It is partitioned accordingly,

$$K = \begin{pmatrix} 0 & K_{IJ} \\ K_{JI} & K_{JJ} \end{pmatrix}, \tag{5}$$

in which $K_{IJ} \in \mathbb{R}^{n\times(N-n)}$, $K_{JI} = K_{IJ}^{\mathrm{T}}$, and $K_{JJ} \in \mathbb{R}^{(N-n)\times(N-n)}$. Since the interaction between the retained atoms is already included in $\Phi$, we assume the first entry to be zero. Similarly since the loading condition is applied at the remote boundary, we assume that

$$\mathbf{f}^{\mathrm{b}} = \begin{pmatrix} 0 \\ \mathbf{f}_J^{\mathrm{b}} \end{pmatrix}.$$

The Hamilton's equations then read,

$$m\ddot{\mathbf{u}}_J = -K_{JJ}\mathbf{u}_J - K_{JI}\mathbf{u}_I + \mathbf{f}_J^{\mathrm{b}}, \tag{6a}$$

$$m\ddot{\mathbf{u}}_I = -K_{IJ}\mathbf{u}_J - \nabla_{\mathbf{u}_I}\Phi. \tag{6b}$$

The initial state of the system is prepared so that the heat bath is in thermal equilibrium, while the atoms in the computational domain are initialized with deterministic data. More precisely, given $(\mathbf{u}_I, \mathbf{v}_I)$, $(\mathbf{u}_J, \mathbf{v}_J)$ are sampled from the Gibbs distribution,

$$\frac{1}{Z}\,\mathrm{e}^{-\beta\mathcal{H}'}, \tag{7}$$

where

$$\mathcal{H}'(\mathbf{u}_J,\mathbf{v}_J)=\frac{1}{2}(\mathbf{u}_J-\bar{\mathbf{u}}_J+K_{JJ}^{-1}K_{JI}\mathbf{u}_I)^{\mathrm{T}}K_{JJ}(\mathbf{u}_J-\bar{\mathbf{u}}_J+K_{JJ}^{-1}K_{JI}\mathbf{u}_I)+\frac{m}{2}(\mathbf{v}_J-\bar{\mathbf{v}}_J)^2. \tag{8}$$

Here, $\beta=(k_{\mathrm{B}}T)^{-1}$ is the inverse temperature, $Z$ is the partition function that normalizes the distribution, $\bar{\mathbf{u}}_J$ and $\bar{\mathbf{v}}_J$ prescribe the initial average displacement and velocity field for the bath. They are assumed to be smooth, i.e. they vary slowly on the atomic scale.

Next, we define the projection operator $\mathcal{P}$ such that for any function $g(\mathbf{u},\mathbf{v})$, we have

$$\mathcal{P}g(\mathbf{u},\mathbf{v})=E[g], \tag{9}$$

where $E[\cdot]$ is the expectation with respect to the normal distribution,

$$\rho(\mathbf{u}_J,\mathbf{v}_J)=\frac{\mathrm{e}^{-\beta\mathcal{H}'(\mathbf{u}_J,\mathbf{v}_J)}}{\int \mathrm{e}^{-\beta\mathcal{H}'(\mathbf{u}_J,\mathbf{v}_J)}d\mathbf{u}_J d\mathbf{v}_J}.$$

In particular, we have

$$\mathcal{P}\varphi(\mathbf{u}_I(0))=\varphi(\mathbf{u}_I(0)) \tag{10}$$

for any function $\varphi$ and

$$\mathcal{P}\mathbf{u}_J(0)=\bar{\mathbf{u}}_J-K_{JJ}^{-1}K_{JI}\mathbf{u}_I(0). \tag{11}$$

Similarly,

$$\mathcal{P}\varphi(\mathbf{v}_I(0))=\varphi(\mathbf{v}_I(0)),\quad \mathcal{P}\mathbf{v}_J=\bar{\mathbf{v}}_J. \tag{12}$$

For the complementary projection operator $\mathcal{Q}$, $\mathcal{Q}=I-\mathcal{P}$, we have

$$\mathcal{Q}\varphi(\mathbf{u}_I(0))=0,\quad \mathcal{Q}\mathbf{u}_J(0)=\mathbf{u}_J(0)-[\bar{\mathbf{u}}_J-K_{JJ}^{-1}K_{JI}\mathbf{u}_I(0)]. \tag{13}$$

The projection operators have been motivated by the optimal prediction method [9,8,10,11], where the operator has been defined as the conditional expectation.

Our next step is to derive the equations only involving the retained variables. First we recall the Liouville operator,

$$\mathcal{L}=\mathbf{v}\cdot\nabla_{\mathbf{u}}-\frac{1}{m}\nabla_{\mathbf{u}}\mathcal{H}\cdot\nabla_{\mathbf{v}}. \tag{14}$$

From (6), we have

$$\mathcal{L}\mathbf{u}=\mathbf{v},\quad \mathcal{L}\mathbf{v}_I=-\frac{1}{m}(K_{IJ}\mathbf{u}_J+\nabla\Phi),\quad \mathcal{L}\mathbf{v}_J=\frac{1}{m}(-K_{JJ}\mathbf{u}_J-K_{JI}\mathbf{u}_I+\mathbf{f}_J^{\mathrm{b}}).$$

The Mori–Zwanzig's procedure [5,42,43,32] yields

$$m\ddot{\mathbf{u}}_I=m\mathrm{e}^{t\mathcal{L}}\mathcal{P}\mathcal{L}\mathbf{v}_I(0)+\int_0^t \mathrm{e}^{\tau\mathcal{L}}K(t-\tau)\mathrm{d}\tau+R(t), \tag{15}$$

where

$$R(t)=m\mathrm{e}^{t\mathcal{Q}\mathcal{L}}\mathcal{Q}\mathcal{L}\mathbf{v}_I(0), \tag{16a}$$

$$K(t)=\mathcal{P}\mathcal{L}R(t). \tag{16b}$$

The procedure involves a decomposition using the projection operators, and the history-dependent term comes from the Dyson's formula. More details can be found in [44]. Equations in the form of (15) are known as the generalized Langevin equations (GLE). The first term on the right hand side describes the interaction among the retained variables. The second term describes history-dependence of the dynamics: After eliminating the degrees of freedom associated with the heat bath, the dynamics is no longer Markovian. The last term, which represents the influence of the heat bath, is often regarded as the random force.

Next, we will compute the terms on the right hand side.

### 2.1. The first term

For the first term on the right hand side of (15), we have

$$m\mathcal{P}\mathcal{L}\mathbf{v}_I(0)=K_{IJ}K_{JJ}^{-1}K_{JI}\mathbf{u}_I(0)-\nabla\Phi(\mathbf{u}_I(0))-K_{IJ}\bar{\mathbf{u}}_J,$$

yielding

$$m\mathrm{e}^{t\mathcal{L}}\mathcal{P}\mathcal{L}\mathbf{v}_I(0)=K_{IJ}K_{JJ}^{-1}K_{JI}\mathbf{u}_I-\nabla\Phi(\mathbf{u}_I)-K_{IJ}\bar{\mathbf{u}}_J. \tag{17}$$

### 2.2. The random force

To compute $R(t)$ explicitly, we observe that at $t = 0$,

$$R(0) = -K_{IJ}[\mathbf{u}_J(0) - (\bar{\mathbf{u}}_J - K_{JJ}^{-1}K_{JI}\mathbf{u}_I)]. \tag{18}$$

This, along with the form of the projection operators, suggests that we seek the random force in the form of

$$R(t) = C(t)[\mathbf{u}_J(0) - (\bar{\mathbf{u}}_J - K_{JJ}^{-1}K_{JI}\mathbf{u}_I(0))] + S(t)(\mathbf{v}_J(0) - \bar{\mathbf{v}}_J), \tag{19}$$

with coefficients $C \in \mathbb{R}^{n\times(N-n)}$ and $S \in \mathbb{R}^{n\times(N-n)}$ to be determined.

Furthermore, from Eq. (16a), one has

$$\dot{R}(t) = \mathcal{Q}\mathcal{L}R(t),$$

which combined with Eq. (19), yields

$$\begin{cases} m\dot{C}(t) = -S(t)K_{JJ}, \\ \dot{S}(t) = C(t), \\ C(0) = -K_{IJ}, \\ S(0) = 0. \end{cases} \tag{20}$$

Here, the initial condition is obtained from (18). From the equations above, one can easily verify that

$$m\ddot{C} = -CK_{JJ}, \quad C(0) = -K_{IJ}, \quad \dot{C}(0) = 0. \tag{21}$$

This defines an exterior problem in the bath region, where the equation is the linearized MD, and comparing to (6), there is no traction applied at the remote boundary or the interface with the computational domain. Furthermore, one observes that the solution of the equation above only depends on the force constants. It is *independent* of the remote boundary condition and the temperature.

Using Eq. (20), one can prove that the random force $R(t)$ is a stationary Gaussian process with zero average. The time correlation is given by

$$\langle R(t+s)R(s)^{\mathrm{T}}\rangle = -k_{\mathrm{B}}TC(t)K_{JJ}^{-1}K_{JI} = k_{\mathrm{B}}T\Theta(t), \tag{22}$$

where we defined the function $\Theta(t) \in \mathbb{R}^{n\times n}$ as follows:

$$\Theta(t) = -C(t)K_{JJ}^{-1}K_{JI}. \tag{23}$$

In particular,

$$\Theta(0) = K_{IJ}K_{JJ}^{-1}K_{JI} \tag{24}$$

is a semi positive–definite matrix. Such relation between the fluctuation of the random force and the memory kernel has been referred to as the second fluctuation–dissipation theorem [24].

### 2.3. The memory term

The memory term will be computed from (16b) and (19). A direct calculation gives

$$K(t) = \mathcal{P}\mathcal{L}R(t) = C(t)\bar{\mathbf{v}}_J - \frac{1}{m}S(t)K_{JJ}\bar{\mathbf{u}}_J + C(t)K_{JJ}^{-1}K_{JI}\mathbf{v}_I(0) + \frac{1}{m}S(t)\mathbf{f}_J^{\mathrm{b}}.$$

With a substitution into (15), we can simplify the memory term to,

$$\int_0^t \mathrm{e}^{\tau\mathcal{L}}K(t-\tau)\mathrm{d}\tau = C(t)\bar{\mathbf{u}}_J + S(t)\bar{\mathbf{v}}_J + (C(0) - C(t))K_{JJ}^{-1}\mathbf{f}_J^{\mathrm{b}} + K_{IJ}\bar{\mathbf{u}}_J - \int_0^t \Theta(\tau)\mathbf{v}_I(t-\tau)\mathrm{d}\tau. \tag{25}$$

### 2.4. The generalized Langevin equation

Finally, by collecting terms, we arrive at the generalized Langevin equation,

$$m\ddot{\mathbf{u}}_I = -\nabla\Phi(\mathbf{u}_I) + \Theta(0)\mathbf{u}_I - \int_0^t \Theta(\tau)\dot{\mathbf{u}}_I(t-\tau)\mathrm{d}\tau + R(t) + \mathbf{f}^{\mathrm{ex}}. \tag{26}$$

Here,

$$\mathbf{f}^{\mathrm{ex}} = C(t)\bar{\mathbf{u}}_J + S(t)\bar{\mathbf{v}}_J + (C(0) - C(t))K_{JJ}^{-1}\mathbf{f}_J^{\mathrm{b}} \tag{27}$$

is regarded as the external force from the surrounding bath, $\Theta(t)$ will be called the memory kernel, and $R(t)$ is a random force.

For each atom in the computational domain, $i \in \mathcal{D}$, the equation above becomes

$$m\ddot{\mathbf{u}}_i = -\nabla_{\mathbf{u}_i}\Phi + \sum_{j\in\mathcal{D}}\left[\theta_{ij}(0)\mathbf{u}_j - \int_0^t \theta_{ij}(\tau)\dot{\mathbf{u}}_j(t-\tau)\mathrm{d}\tau\right] + R_i(t) + \mathbf{f}_i^{\mathrm{ex}}. \tag{28}$$

It has been shown in [27] that the memory and random force terms will be zero for atoms whose distance to the boundary is larger than the cut-off radius. Therefore, these terms will only appear for atoms near the boundary.

### 2.5. The connection with the lattice Green's functions

Another approach to derived the boundary condition is based on the lattice Green's function, e.g. see [23]. Here we will make the connection between these two methods.

The main idea is to solve (6a) first, and then substitute it into (6b). To begin with, we consider the following problem:

$$m\ddot{\mathbf{w}} = -K_{JJ}\mathbf{w}, \quad \mathbf{w} \in \mathbb{R}^{N-n} \tag{29}$$

with initial condition $\mathbf{w}(0)$ and $\dot{\mathbf{w}}(0)$. As discussed in the previous section, this defines an exterior problem in the bath with no forces applied at the boundaries.

To find the solution of this system, we define the following Green's functions, $G(t) \in \mathbb{R}^{(N-n)\times(N-n)}$, satisfying the equation:

$$\begin{cases} m\ddot{G} = -K_{JJ}G, \\ G(0) = 0, \quad \dot{G}(0) = I. \end{cases} \tag{30}$$

Taking the time derivative, and letting $H = \dot{G}$, we have

$$\begin{cases} m\ddot{H} = -K_{JJ}H, \\ H(0) = I, \quad \dot{H}(0) = 0. \end{cases} \tag{31}$$

Applying Laplace transform, one gets

$$\widehat{G}(\lambda) = [\lambda I + K_{JJ}]^{-1}, \quad \widehat{H}(\lambda) = \lambda[\lambda I + K_{JJ}]^{-1}.$$

Thus using the Green's functions, we can express the solution to the exterior problem (29) as

$$\mathbf{w}(t) = \dot{G}(t)\mathbf{w}(0) + G(t)\dot{\mathbf{w}}(0). \tag{32}$$

Especially by comparing (30) and (31) with (20), we get

$$C(t) = -K_{IJ}\dot{G}(t), \quad S(t) = -K_{IJ}G(t). \tag{33}$$

To make connections to the GLE (26), we will split the problem into several subproblems. First we consider the case when the system is in mechanical equilibrium, but is connected to the computational domain

$$\begin{cases} m\frac{d^2}{dt^2}\mathbf{u}_J^{(1)} = -K_{JJ}\mathbf{u}_J^{(1)} - K_{JI}\mathbf{u}_I, \\ \mathbf{u}_J^{(1)}(0) = -K_{JJ}^{-1}K_{JI}\mathbf{u}_I(0), \quad \frac{\mathrm{d}}{\mathrm{d}t}\mathbf{u}_J^{(1)}(0) = 0. \end{cases} \tag{34}$$

The bath is in mechanical equilibrium since

$$K_{JJ}\mathbf{u}_J^{(1)}(0) + K_{JI}\mathbf{u}_I(0) = 0.$$

Applying Laplace transform, one finds

$$\mathbf{u}_J^{(1)}(t) = -\dot{G}(t)K_{JJ}^{-1}K_{JI}\mathbf{u}_I(0) + \int_0^t \boldsymbol{\alpha}(\tau)\mathbf{u}_I(t-\tau)\mathrm{d}\tau, \tag{35}$$

where

$$\hat{\boldsymbol{\alpha}}(\lambda) = -[\lambda I + K_{JJ}]^{-1}K_{JI}.$$

Therefore,

$$\boldsymbol{\alpha}(t) = -G(t)K_{JI}. \tag{36}$$

In addition, the influence on the atoms in $\mathcal{D}$ is given by

$$-K_{IJ}\mathbf{u}_J^{(1)}(t) = \Theta(0)\mathbf{u}_I(t) - \int_0^t \Theta(\tau)\dot{\mathbf{u}}_I(t-\tau)\mathrm{d}\tau, \tag{37}$$

where

$$\Theta(t) = -K_{IJ}\int_t^{+\infty} \boldsymbol{\alpha}(\tau)\mathrm{d}\tau. \tag{38}$$

This produces the memory term in the GLE (26), and in light of (33), the memory functions defined in (23) and (38) are the same.

To include the random noise from the heat bath, we consider the following subproblem:

$$\begin{cases} m\frac{\mathrm{d}^2}{\mathrm{d}t^2}\mathbf{u}_J^{(2)} = -K_{JJ}\mathbf{u}_J^{(2)} \\ \mathbf{u}_J^{(2)}(0) \sim \mathcal{N}(0, k_\mathrm{B}TK_{JJ}^{-1}), \quad \mathbf{v}_J^{(2)}(0) \sim \mathcal{N}(0, k_\mathrm{B}T/mI). \end{cases} \tag{39}$$

Namely, the initial condition is picked from the Gaussian distribution,

$$\frac{1}{Z}\mathrm{e}^{-\beta\left(\frac{1}{2}\mathbf{u}_J^{\mathrm{T}}K_{JJ}\mathbf{u}_J + \frac{1}{2}m\mathbf{v}_J^2\right)}.$$

The solution to this problem is given by (32). The substitution into (6b) yields

$$-K_{IJ}\mathbf{u}_J^{(2)}(t),$$

which can be identified to be the random noise term using (33) and (18).

The third subproblem picks up the existing elastic field and the remote boundary condition:

$$\begin{cases} m\frac{\mathrm{d}^2}{\mathrm{d}t^2}\mathbf{u}_J^{(3)} = -K_{JJ}\mathbf{u}_J^{(3)} + \mathbf{f}_J^{\mathrm{b}}, \\ \mathbf{u}_J^{(3)}(0) = \bar{\mathbf{u}}_J, \quad \frac{\mathrm{d}}{\mathrm{d}t}\mathbf{u}_J^{(3)}(0) = \bar{\mathbf{v}}_J. \end{cases} \tag{40}$$

Using Laplace transform, one finds the solution

$$\mathbf{u}_J^{(3)} = \dot{G}(t)\bar{\mathbf{u}}_J + G(t)\bar{\mathbf{v}}_J + (\dot{G}(0) - \dot{G}(t))K_{JJ}^{-1}\mathbf{f}_J^{\mathrm{b}},$$

which combined with (33) and (27), recovers the external force $\mathbf{f}_J^{\mathrm{ex}}$.

Finally, we get

$$\mathbf{u}_J = \mathbf{u}_J^{(1)} + \mathbf{u}_J^{(2)} + \mathbf{u}_J^{(3)},$$

which satisfies (6a) with the correct initial and boundary conditions, and the substitution into (6b) gives the GLE (26).

## 3. Modeling the external loading

### 3.1. Pressure bath

One common approach to introduce the external loading is to prepare the system by selecting initial conditions from an existing elastic field which is already in equilibrium. In this case, we have

$$-K_{JJ}\bar{\mathbf{u}}_J - K_{JI}\mathbf{u}_I(0) = 0, \quad \bar{\mathbf{v}}_J = 0.$$

The external force then becomes

$$\mathbf{f}^{\mathrm{ex}} = C(t)\bar{\mathbf{u}}_J = -C(t)K_{JJ}^{-1}K_{JI}\mathbf{u}_I(0) = \Theta(t)\mathbf{u}_I(0) \tag{41}$$

using (23). Thus the external force term can also be computed using the memory kernel.

For instance, one can deform the bath region with a uniform strain, $\epsilon$. Namely

$$\bar{\mathbf{u}}_j = \mathbf{u}_0 + \boldsymbol{\epsilon}(\mathbf{z}_j - \mathbf{z}_0)$$

for $j \in \mathcal{B}$, and

$$\mathbf{u}_i(0) = \mathbf{u}_0 + \boldsymbol{\epsilon}(\mathbf{z}_i - \mathbf{z}_0)$$

for $i \in \mathcal{D}$. Such idea has been used in the crack simulation [19] to model a uniformly strained system. More generally, since we expect $\bar{\mathbf{u}}_J$ to be smooth, we can use anisotropic solutions obtained from elasticity equations, e.g. the analytical solution for an elliptical crack [36], which has been used in numerous crack simulations [7,28,31,41], and the Stroh's solution [37] for single dislocations.

### 3.2. Remote loading condition

Here we discuss how to model loading condition from far field boundaries. From Section 2.5, we have shown that we can decompose the solution in the bath into three parts

$$\mathbf{u}_J = \mathbf{u}_J^{(1)} + \mathbf{u}_J^{(2)} + \mathbf{u}_J^{(3)},$$

in which $\mathbf{u}_J^{(1)}(t)$ is the solution of (34), represented by the memory term in the GLE (26), and $\mathbf{u}_J^{(2)}(t)$ is the solution of (39) which corresponds to the random force. They can be computed once the memory kernel is available.

The third part $\mathbf{u}_J^{(3)}$ includes the loading condition from the remote boundary and the initial elastic field. In the case where the initial and boundary conditions are smooth, we expect the solution to be smooth. In this case, Eq. (40) can be replaced by a continuum elastodynamics equation:

$$\rho_0 \frac{\partial^2}{\partial t^2}\mathbf{u} = \nabla \cdot \boldsymbol{\sigma}, \tag{42}$$

where $\rho_0$ is the density in the reference coordinate. To make the continuum models consistent with the underlying atomistic model, the stress, $\boldsymbol{\sigma}$, should be computed from the interatomic potential. Typically, this done using either the Cauchy–Born rule [16], or a linear stress–strain relation with elastic moduli computed from the atomistic models. For instance the idea of approximating molecular dynamics by elasticity models has been investigated in [15]; Since in our bath region, the atomic interaction has been linearized, we will use the anisotropic linear elasticity model with elastic parameters computed from the force constant [4]

$$c_{\alpha\mu\beta\nu} = -\frac{1}{8V_0}\sum_i z_i^\alpha K_i^{\mu\nu} z_i^\beta + z_i^\mu K_i^{\alpha\nu} z_i^\beta + z_i^\alpha K_i^{\mu\beta} z_i^\nu + z_i^\mu K_i^{\alpha\beta} z_i^\nu, \tag{43}$$

where $V_0$ is the volume of a unit cell, the superscripts indicate the entries and summation is over a neighborhood of the origin within the cut-off radius.

**Remark 1.** Clearly more general remote loading conditions, such as dead loading or dynamic loading condition can also be dealt with using this method.

**Remark 2.** This idea is quite similar to conventional domain decomposition method. However, we would not perform iterations between the two regions because the molecular dynamics simulation is already quite expensive. Instead, the memory kernel, which is analogous to the Dirichlet-to-Neumann map, offers the accurate coupling condition.

## 4. Approximating the memory kernel: variational boundary condition

In order to solve the generalized Langevin equation (26), one has to find the kernel function $\Theta(t)$, which will in turn determine the random force since $R(t)$ is Gaussian and stationary. Although in principle, this function can be computed from (20), it would not be practical for the following reasons:

1. the system (20) is rather large, the computation could be as expensive as solving the full system (1);
2. the memory kernel obtained from this approach is exact. But it is usually rather non-local in that it involves all the atoms at the boundary, and their previous history. Directly implementing such kernels will dramatically slow down the simulation.

Therefore, it is of practical interest to find approximate kernels that are local and at the same time, offers reasonable accuracy. The need to approximate the Mori–Zwanzig formalism has also been recognized by Chorin and coworkers in their recent work on optimal prediction [10,8,9]. In this paper, we will use the variational boundary condition (VBC) [26,27]. Here, we will briefly describe the formulation of VBC.

First from the derivations in the previous section we observe that the memory kernel is *independent* of the temperature and the loading condition. In fact as indicated by (33), the function $C(t)$, which subsequently determines $\Theta(t)$, can be obtained from the Green's functions, which only depends on the geometry of the boundary and the force constant. This, however, might not be true if the projection operator is chosen differently [44]. Based on this observation, we will compute the memory kernel at zero temperature with no external loading, in which case the phonons will only emanate from the computational domain and the problem becomes preventing reflections at the boundary. In fact it has been shown that for the exact memory kernel, the reflection coefficient is zero for all phonon mode [27]. After the memory kernel is obtained, the random noise will be sampled based on the fluctuation–dissipation theorem.

The variational formulation aims to find a memory kernel in the form of

$$\Theta(t) = \int_{-\infty}^{+\infty} \Gamma(\tau)\Gamma(t+\tau)^{\mathrm{T}}\,\mathrm{d}\tau. \tag{44}$$

To make the kernel local, we require that the function $\Gamma(t)$ must have compact support on some finite interval $[0, t_0]$. In space, the is done by requiring that each entry $\theta_{ij}$ be non-zero only for those atoms $j$ that are close to atom $i$, and these preselected atoms will be called the *stencil*. The purpose of expressing the kernel $\Theta(t)$ in this particular form is two-fold: first, such memory kernel guarantees the numerical stability [25]. Secondly, the Gaussian process, $R(t)$, can be easily constructed from $\Gamma(t)$. More specifically, let $W(t)$ be the white noise, i.e.

$$\langle W_p(t+s)W_q(s)^{\mathrm{T}}\rangle = \delta_{pq}\delta(t) \quad \text{for any } s \geqslant 0.$$

Then the random force can be sampled as follows:

$$R(t) = \sqrt{k_{\mathrm{B}}T}\int_{-\infty}^{+\infty} \Gamma(\tau)W(t-\tau)\mathrm{d}\tau. \tag{45}$$

One can easily verify that the fluctuation–dissipation theorem (22) is satisfied.

In order to find the memory kernel with optimal accuracy, we define the total reflection as

$$E[\{\Gamma_j\}; \mathbf{n}] = \sum_s \sum_{s'} \int |B_{ss'}|^2 W_s(\mathbf{k})\mathrm{d}\mathbf{k}, \tag{46}$$

where $\mathbf{k}$ is a phonon mode, $W_s(\mathbf{k}) \geqslant 0$ is some weight function, and the integration is over the Brillouin zone [4]. $B_{ss'}(\mathbf{k})$, which can be computed from the memory kernel $\Gamma(t)$, is the coefficient of reflection from branch $s$ to $s'$. Here since the bath region is much larger, we will treat it as an infinite medium, and we only take into account the reflection off the interface with the computational domain.

There are many natural choices of the weight function $W$. In [13,14], $W$ is taken to be a constant. In [26], $W$ is taken as

$$W_s(\mathbf{k}) = |\nabla\omega_s(\mathbf{k})\cdot\mathbf{n}|. \tag{47}$$

In this case, Eq. (46) represents the energy flux across the boundary due to the reflection of phonons.

Finally, the local boundary condition is found by minimizing the total reflection (46).

The overall numerical procedure can be summarized as follows:

(1) compute the memory kernel from the variational formulation,
(2) compute the random noise from (45),
(3) approximate $\mathbf{u}_j^{(3)}(t)$ by solving the continuum Eq. (42), and compute the force on the atoms in the computational domain, $\mathbf{f}^{\mathrm{ex}} = -K_{IJ}\mathbf{u}_J^{(3)}(t)$,
(4) solve the generalized Langevin equation (26).

## 5. Examples

### 5.1. A one-dimensional chain model

As the first example, we consider a one-dimensional chain of atoms connected by springs

$$m\ddot{r}_j = \varphi'(r_{j+1} - r_j) - \varphi'(r_j - r_{j-1}). \tag{48}$$

Here, $m$ is the mass of an atom, $r_j$ denotes the position, and $\varphi$ is the interatomic potential. The equilibrium configuration of the system be given by $z_j = ja_0$ with $a_0$ being the lattice parameter. The spectrum of the discrete lattice waves, known as phonons, can be obtained by linearizing Eq. (48), yielding

$$m\ddot{u}_j = K(u_{j+1} - 2u_j + u_{j-1})/a_0^2, \tag{49}$$

where $u_j = r_j - z_j$ is the displacement, and $K = \varphi''(a_0)a_0^2$.

For this model, if the whole left half is regarded as the bath, the memory kernel can be computed explicitly [1,2],

$$\theta(t) = \frac{\sqrt{m}\,K}{t}J_1\left(\frac{2Kt}{\sqrt{m}}\right),$$

where $J_1$ is the Bessel function of the first kind.

In our computation we non-dimensionalize the system (48) and all the numerical results will be provided with $\{K, m, a_0\}$ as energy, mass and length unit, respectively. For the atomic potential, we use the Lennard–Jones potential,

$$\varphi(r) = 4((1/r)^{12} - (1/r)^6). \tag{50}$$

The numerical experiment is set up as follows: We restrict the computational domain to the right half of the system, $j > 0$. This is shown in Fig. 2. The atoms in the computational domain are initially at rest, while the atoms in the bath region, i.e. for $j \leqslant 0$, is uniformly deformed with strain $\varepsilon = 0.01$. Namely the initial displacement is given by,


**Fig. 2.** A schematic of the boundary: filled circles represent the selected atoms that will be followed in the computation; open circles are the atoms outside. The boundary is between the zeroth atom and the first atoms.

$$u_j(0) = \begin{cases} 0, & \text{if } j \geqslant 0, \\ j\varepsilon, & \text{if } j < 0. \end{cases}$$

The initial velocity is zero for every atom.

The computational domain consists of 100 atoms, and we choose the time step $\Delta t = 0.2$. For the memory kernel $\Gamma(t)$ in (44), we pick $t_0 = 4$. Using the boundary condition, the system is evolved for 200 time steps, and Fig. 3 displays numerical results, which agree with the exact solutions, also shown in the figure. The exact solution is computed from a full simulation which involves the bath atoms explicitly.

### 5.2. Simulation of cracks in 3D iron-α system

Next, we consider a more realistic example, a model of α-iron, which is a three-dimensional BCC system. The atomic potential used is the embedded atom potential developed in [35]. The system studied is a 3D rectangular sample, with the three orthogonal axes along the $[1\,1\,0]$, $[1\,\bar{1}\,0]$ and $[0\,0\,1]$ directions, respectively. The system has the dimension of $60 \times 30 \times 6$ atomic units, containing 43,600 atoms. The crack is formed by removing a few atoms at the center row. Here, we will use physical units. The mass, length and energy units are chosen to be 55.845 a.m.u. (atomic mass unit), Å (Angstrom) and $k_B$ K ($1.38065 \times 10^{-23}$ J), respectively. The corresponding time scale is 8.19 ps. In all the following simulations, we set the time step to $\Delta t = 0.002$.

We will study a center cracked system under mode I loading, shown in Fig. 4. For the computational domain, variational boundary condition is applied to the top and bottom boundaries, while in the horizontal direction, periodic boundary condition is used. For the memory kernel, we choose the spatial stencil to consist of 25 atoms, with 5 atoms in each tangential direction, and we set $t_0 = 0.04$.

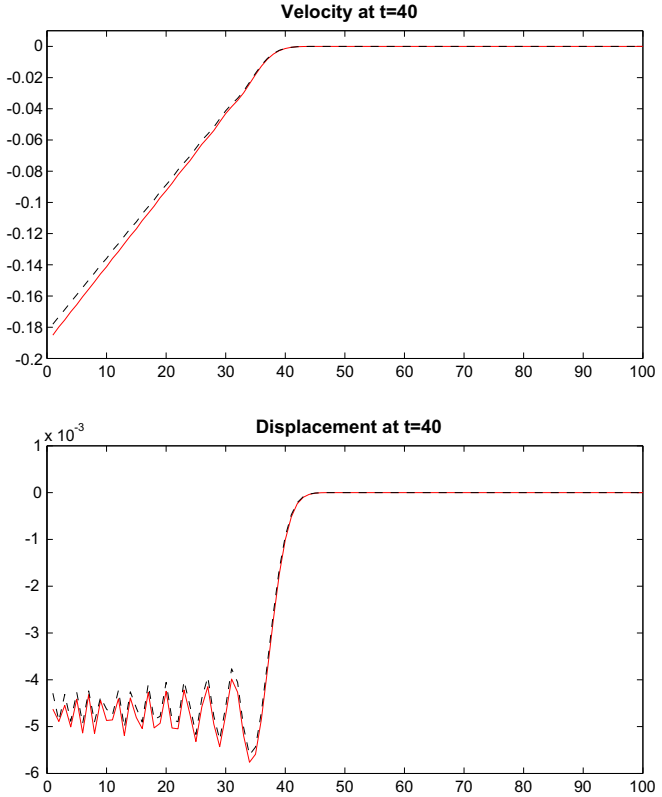


**Fig. 3.** The displacement and velocity of the atoms at $t = 40$. Solid line: exact solution; dashed line: solution obtained from variational boundary condition.

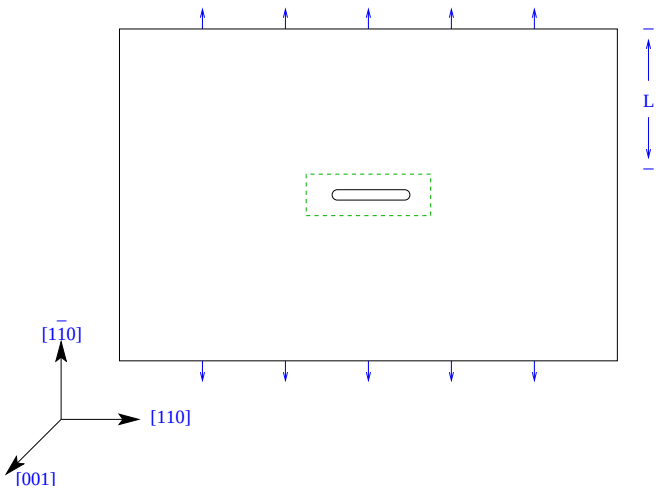


**Fig. 4.** Setup of the simulation: a centered crack under mode I loading. The computational domain is inside the dashed line.

In the first test, the bath is under a uniaxial strain, $\varepsilon_{22} = 0.0027$ while the computational domain is at rest initially. The numerical results are displayed in Fig. 5 for different values of the applied temperature. We plot the position of the atoms from a cross section of the $\langle 0\,0\,1\rangle$ plane. We observe that at $T = 0$ K, and $T = 250$ K, the crack does not open up. However, at $T = 500$ K, the crack grows slightly and then dislocations appear in the [1 0 0] direction and move away from the crack tip.

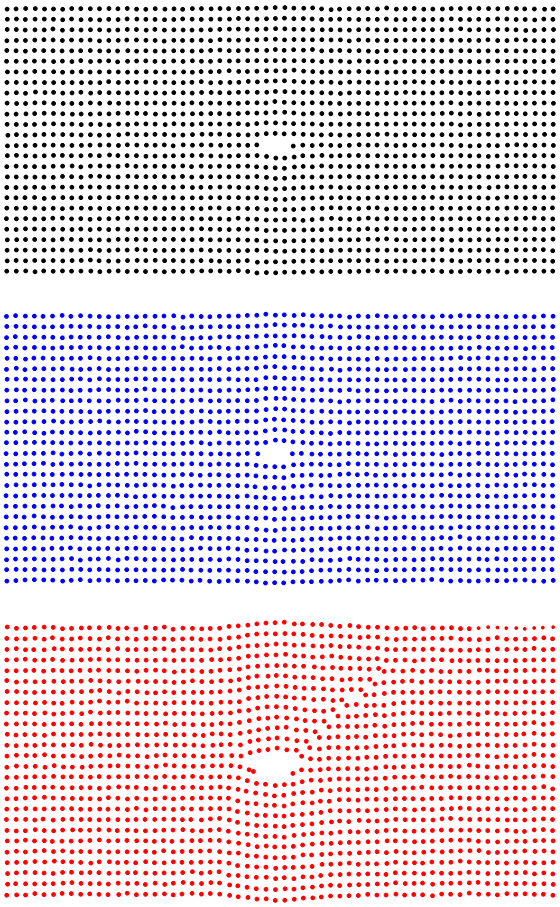

**Fig. 5.** Simulation of a crack: the position the atoms at $t = 40$. From top to bottom: $T = 0$ K $T = 250$ K; $T = 500$ K.

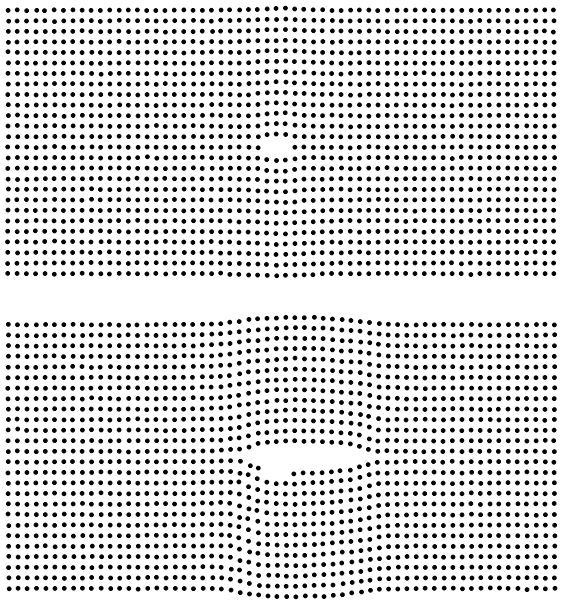

**Fig. 6.** Crack under uniaxial strain. Top: $\varepsilon_{22} = 0.0031$, the solution is plotted at $t = 80$ (0.655 ns); bottom: $\varepsilon_{22} = 0.0032$, the solution is plotted at $t = 10$ (0.082 ns).

Next we keep the temperature at $T = 0$ K, and increase the strain to $\varepsilon_{22} = 0.031$ and $\varepsilon_{22} = 0.032$, and the results are shown in Fig. 6. We see that at $\varepsilon_{22} = 0.031$, the crack does not move forward even after a long time integration. However, at $\varepsilon_{22} = 0.032$, the crack starts to propagate without generating dislocations. In addition we have observed similar behavior as in the previous test if we raise the temperature to 500 K. This indicates that the crack in this material is brittle at zero temperature, and ductile at higher temperature $T = 500$ K. This agrees with the results observed in [7].

In the last experiment, we study the system under remote dynamic loading condition. The whole sample is initially at rest, and at the top remote boundary, the velocity is prescribed at follows:

$$v_2(x, L, t) = \begin{cases} v_0 t/t_0 & \text{if } t \leqslant t_0, \\ v_0 & \text{if } t > t_0. \end{cases} \tag{51}$$

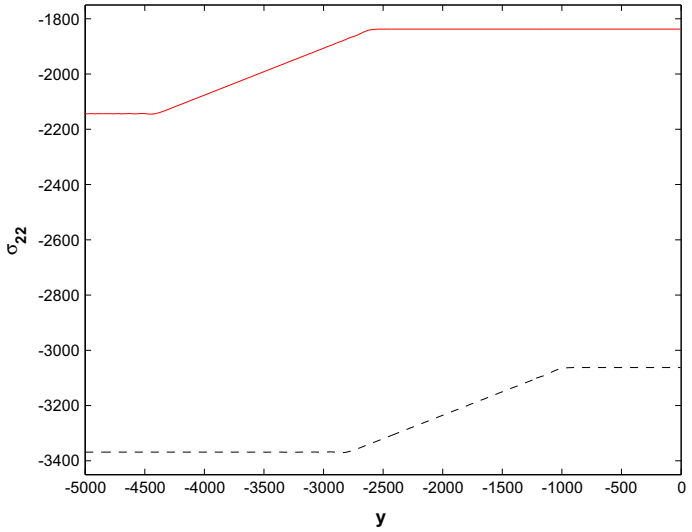


**Fig. 7.** Stress waves generated from the bottom boundary condition. Solid line: $t = 72$(0.590 ns), the magnitude of the stress wave is 2143 (29.59 GPa); Dashed line: $t = 120$ (0.981 ns), the magnitude of the stress wave is 3368 (46.51 GPa).

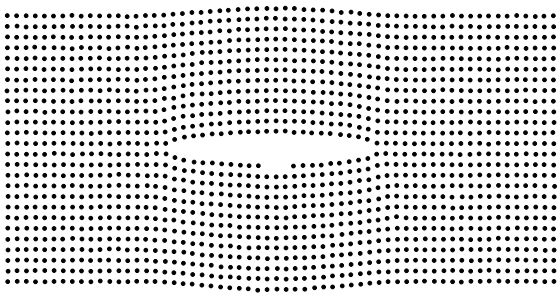

**Fig. 8.** Crack under dynamic loading. The solution is plotted at $t = 144$ (1.18 ns).

We choose $v_0 = 8(97.68\ \mathrm{ms}^{-1}), t_0 = 10(81.9\ \mathrm{ps})$, and the size of the bath region $L = 5000$ (0.5 μm). The boundary condition at the bottom is applied in the same way with opposite direction. The setup of this simulation is motivated by the fracture simulation [33]. Since the system is periodic in the other two directions, we replace the elastodynamics (42) with a one-dimensional model

$$\rho_0 \frac{\partial^2}{\partial t^2} u_2 = C_{11} \frac{\partial^2}{\partial y^2} u_2.$$

Here $\rho_0 = 0.08493$ $(7.869\ g\ cm^{-3})$ and $C_{11} = 17253.37\ k_B K\ \text{Å}^{-3}$ (238.2 GPa), both computed from the atomistic model. The equation is solved by a finite difference method.

Fig. 7 shows the incident stress waves at $t = 72$ and $t = 120$, and under the second stress wave, the crack starts to open. A snapshot of the system at $t = 144$ (1.18 ns) is displayed in Fig. 8.

## 6. Summary and discussion

We have presented a theoretical framework for deriving the boundary conditions for molecular dynamics simulations of crystalline solids at finite temperature with external loading conditions. In addition we have presented practical applications of this framework. In contrast to empirical methods, the current approach is more first principle-based: It starts with the full atomistic description, and the Mori–Zwanzig formalism is used to eliminate the bath atoms and derive the effective boundary condition in the form of GLEs. We have discussed how to compute the external force, which appears in the GLEs as a result of the loading conditions.

The primary purpose of these boundary conditions is to model the influence from the surrounding bath and the loading condition at the remote boundaries. With these boundary conditions, one can conduct simulations without having to treat the bath atoms explicitly. For the examples in the previous section, full simulations would have to be several times larger in order to eliminate the boundary effect. They will be even more impractical for the finite temperature case, because the initial condition in the bath is extremely difficult to prepare. This computational gain will be much greater for more complicated problems, e.g. the interaction of local defects with elastic waves. The variational boundary condition further reduces the computational cost by using local kernel functions.

Our formulation is based on the assumption that the atomic interaction involving the atoms in the bath is linear. This is a reasonable approximation for prefect crystal. But it will prevent the local defect from entering the bath, e.g. a dislocation propagating through the boundary observed in the second numerical example. This is the main limitation of these boundary conditions.

The current method can be applied to an isolated molecular dynamics simulation, as demonstrated in this paper. Moreover it can be applied to a multiscale method that involves both atomistic and continuum models in the simulation. In this case, the GLEs provide the boundary condition at the interface as the coupling strategy. The continuum variables provide the loading condition on the atomistic region. This work is in progress.

Another extension of the current method is to coarse-grain a molecular system. More specifically, instead of dividing the system into two separate domains, one selects a set of representative atoms throughout the domain, which is similar to the setup of the quasi-continuum method [38]. Then, Mori–Zwanzig formalism can be used to derive the effective equations for these selected atoms, reducing the atomic degrees of freedom dramatically. In this case, many interesting issues arise, such as the ghost force, energy conservation, and the calculation of the random noise and memory terms, etc. These issues will be addressed in separate works.

## Appendix A. Simplifying the atomic potential

Here we show how the harmonic approximation can be made to arrive at a simplified model for the atomic potential. As shown in Fig. 1, the computational domain, $\Omega$, is divided into the computational domain, $\mathcal{D}$, and the bath region, $\mathcal{B}$,

$$\Omega = \mathcal{D} \cup \mathcal{B}.$$

We consider the potential energy from the embedded atom model (EAM) [12],

$$V = \frac{1}{2}\sum_{i\neq j}\varphi(\mathbf{r}_{ij}) + \sum_i E(\rho_i), \quad \rho_i = \sum_{j\neq i}\rho(\mathbf{r}_{ij}), \quad \mathbf{r}_{ij} = \mathbf{r}_i - \mathbf{r}_j. \tag{A.1}$$

The function $\varphi$ and $\rho$ only depends on the interatomic distance. Namely, $\varphi(\mathbf{r}) = p(r)$, with $r = |\mathbf{r}|$, then

$$\nabla\varphi = p'\frac{\mathbf{r}}{r}, \quad \nabla^2\varphi = (p'' - p'/r)\frac{\mathbf{r}\otimes\mathbf{r}}{r^2} + p'/rI.$$

It is easy to compute the force on an atom $i$ in the interior of the system,

$$-\nabla_{\mathbf{r}_i}V = -\sum_{j\neq i}\nabla\varphi(\mathbf{r}_{ij}) + (E'(\rho_i) + E'(\rho_j))\nabla\rho(\mathbf{r}_{ij}) \tag{A.2}$$

and the force constants

$$K_{ij} = \nabla^2_{\mathbf{r}_i,\mathbf{r}_j}V = -\nabla^2\varphi(z_{ij}) - 2E'(\rho)\nabla^2\rho(z_{ij}) + E''(\rho)\sum_{k\neq i,k\neq j}\nabla\rho(z_{ik})\otimes\nabla\rho(z_{jk}) \tag{A.3}$$

and

$$K_{ii} = \nabla^2_{\mathbf{r}_i,\mathbf{r}_i}V = \sum\nolimits_{j\neq i}\nabla^2\varphi(z_{ij}) + 2E'(\rho)\nabla^2\rho(z_{ij}) + E''(\rho)\nabla\rho(z_{ij})\otimes\nabla\rho(z_{ij}). \tag{A.4}$$

One can verify that [4],

$$K_{ii} = -\sum_{j\neq i}K_{ij}. \tag{A.5}$$

The force constant, which is second derivatives of the atomic potential at the equilibrium position, will determine the spectrum of the lattice waves, known as phonons [4].

We approximate the atomistic model with a simpler model, which is set up based on the following principles,

(1) The interaction in the heat bath is linear.
(2) The non-linear atomic interaction should be retained in the computational domain $\mathcal{D}$.
(3) At the equilibrium state, the force on each atom should be zero.
(4) The new potential energy has the same phonon spectrum as the original potential model.

We seek the approximate potential in the following form:

$$V_{\text{new}} = V_{\mathcal{D}} + V_{\mathcal{B}},$$

and we will construct these energies separately.

To begin with we construct $V_{\mathcal{B}}$ by the classical harmonic approximation [4],

$$V_{\mathcal{B}} = -\frac{1}{4}\sum_{i\in\mathcal{B},j\in\Omega}(\mathbf{u}_i - \mathbf{u}_j)^{\mathrm{T}}K_{ij}(\mathbf{u}_i - \mathbf{u}_j). \tag{A.6}$$

Meanwhile, the energy $V_{\mathcal{D}}$ is approximated by assuming the distance to the atoms in the bath are at equilibrium,

$$\begin{cases} V_{\mathcal{D}} = \frac{1}{2}\sum\limits_{i\in\mathcal{D},j\in\mathcal{D}}\varphi(\mathbf{r}_{ij}) + \sum\limits_{i\in\mathcal{D}}E(\rho_i) \\ \qquad + \sum\limits_{i\in\mathcal{D},j\in\mathcal{B}}F_{ij}\cdot\mathbf{u}_i - \frac{1}{4}\sum\limits_{i\in\mathcal{D},j\in\Omega}(\mathbf{u}_i - \mathbf{u}_j)^{\mathrm{T}}H_{ij}(\mathbf{u}_i - \mathbf{u}_j), \\ \rho_i = \sum\limits_{j\in\mathcal{D},j\neq i}\rho(\mathbf{r}_{ij}) + \sum\limits_{j\in\mathcal{B}}\rho(z_{ij}). \end{cases} \tag{A.7}$$

Notice that two additional terms have been added to account for the truncation. In these two terms, the constants, $F_{ij}$ and $H_{ij}$, will be selected according to the conditions postulated above. In particular, since the force on each atom $i \in \mathcal{D}$ is given by

$$\nabla_{\mathbf{r}_i}V_{\text{new}} = \sum_{j\neq i,j\in\mathcal{D}}\nabla\varphi(\mathbf{r}_{ij}) + (E'(\rho_i) + E'(\rho_j))\nabla\rho(\mathbf{r}_{ij}) + \sum_{j\in\mathcal{B}}F_{ij} - \frac{1}{2}\sum_{j\in\mathcal{D}}H_{ij}(\mathbf{u}_i - \mathbf{u}_j) - \frac{1}{2}\sum_{j\in\mathcal{B}}(K_{ij} + H_{ij})(\mathbf{u}_i - \mathbf{u}_j). \tag{A.8}$$

From the third assumption, one has

$$F_{ij} = -\nabla\varphi(R_{ij}) - 2E'(\rho)\nabla\rho(z_{ij}) \tag{A.9}$$

by setting $\mathbf{u}_i = \mathbf{u}_j = 0$.

Next, the matrices $H_{ij}$ will be determined from the forth assumption, which suggests that

$$\nabla^2_{\mathbf{r}_i,\mathbf{r}_j} V = \nabla^2_{\mathbf{r}_i,\mathbf{r}_j} V_{\text{new}} \tag{A.10}$$

at the equilibrium position for all $i$ and $j$. In light of (A.6) this certainly is true for $i \in \mathcal{B}$ and $j \in \mathcal{B}$.

On the other hand, for $i \in \mathcal{B}$, we get

$$\nabla_{\mathbf{r}_i} V_{\mathcal{B}} = -\frac{1}{2}\sum_{j\in\Omega} K_{ij}(\mathbf{u}_i - \mathbf{u}_j) - \frac{1}{2}\sum_{j\in\mathcal{B}} K_{ij}(\mathbf{u}_i - \mathbf{u}_j) \tag{A.11}$$

and

$$\nabla_{\mathbf{r}_i} V_{\mathcal{D}} = -\frac{1}{2}\sum_{j\in\mathcal{D}} H_{ij}(\mathbf{u}_i - \mathbf{u}_j). \tag{A.12}$$

As a result for $j \in \mathcal{D}$, we have

$$\nabla^2_{\mathbf{r}_i,\mathbf{r}_j} V_{\text{new}} = \frac{1}{2}(K_{ij} + H_{ij}).$$

Hence, we set

$$H_{ij} = K_{ij} \quad \text{for } i \in \mathcal{D},\ j \in \mathcal{B}.$$

Next, for $i \in \mathcal{D}$ and $j \in \mathcal{D}$, we have

$$\begin{aligned}\nabla^2_{\mathbf{r}_i,\mathbf{r}_j} V_{\mathcal{D}} = H_{ij} &- \nabla^2\varphi(z_{ij}) - 2E'(\rho)\nabla^2\rho(z_{ij}) + E''(\rho)\sum_{k\neq i,k\neq j,k\in\mathcal{D}} \nabla\rho(z_{ik})\otimes\nabla\rho(z_{jk}) + E''(\rho)\nabla\rho(z_{ij})\\ &\otimes\left(\sum_{k\in\mathcal{D},k\neq j}\nabla\rho(z_{jk}) - \sum_{k\in\mathcal{D},k\neq i}\nabla\rho(z_{ik})\right).\end{aligned} \tag{A.13}$$

In addition,

$$\begin{aligned}\nabla^2_{\mathbf{r}_i,\mathbf{r}_i} V_{\mathcal{D}} = H_{ii} &+ \sum_{j\neq i,j\in\mathcal{D}} \nabla^2\varphi(z_{ij}) + 2E'(\rho)\nabla^2\rho(z_{ij}) + E''(\rho)\sum_{j\in\mathcal{D},j\neq i}\nabla\rho(z_{ij})\otimes\sum_{j\in\mathcal{D},j\neq i}\nabla\rho(z_{ij}) + E''(\rho)\sum_{j\in\mathcal{D},j\neq i}\nabla\rho(z_{ij})\\ &\otimes\nabla\rho(z_{ij}).\end{aligned} \tag{A.14}$$

In light of Eqs. (A.4), (A.3) and (A.10), we find that

$$H_{i,j} = E''(\rho)\sum_{k\in\mathcal{B}}\nabla\rho(z_{ik})\otimes\nabla\rho(z_{jk}) + E''(\rho)\nabla\rho(z_{ij})\otimes\left(\sum_{k\in\mathcal{B}}\nabla\rho(z_{jk}) - \sum_{k\in\mathcal{B}}\nabla\rho(z_{ik})\right)$$

and

$$H_{i,i} = \sum_{j\in\mathcal{B}}\nabla^2\varphi(z_{ij}) + 2E'(\rho)\nabla^2\rho(z_{ij}) + E''(\rho)\sum_{j\in\mathcal{B}}\nabla\rho(z_{ij})\otimes\nabla\rho(z_{ij}) - E''(\rho)\sum_{j\in\mathcal{B}}\nabla\rho(z_{ij})\otimes\sum_{j\in\mathcal{B}}\nabla\rho(z_{ij}).$$

Finally, we arrive at the simplified model (4). In particular,

$$\begin{aligned}&\Phi(\mathbf{u}_I) = \frac{1}{2}\sum_{i\in\mathcal{D},j\in\mathcal{D}}\varphi(\mathbf{r}_{ij}) + \sum_{i\in\mathcal{D}}E(\rho_i) + \sum_{i\in\mathcal{D},j\in\mathcal{B}}F_{i,j}\cdot\mathbf{u}_i - \frac{1}{4}\sum_{i\in\mathcal{D},j\in\mathcal{D}}(\mathbf{u}_i-\mathbf{u}_j)^{\mathrm{T}}H_{i,j}(\mathbf{u}_i-\mathbf{u}_j) - \frac{1}{2}\sum_{i\in\mathcal{D}}\mathbf{u}_i^{\mathrm{T}}\left(\sum_{j\in\mathcal{B}}K_{ij}\right)\mathbf{u}_{\mathbf{i}},\\ &\rho_{\mathbf{i}} = \sum\nolimits_{\mathbf{j}\in\mathcal{D},\mathbf{j}\neq\mathbf{i}}\rho(\mathbf{r}_{\mathbf{ij}}) + \sum_{\mathbf{j}\in\mathcal{B}}\rho(\mathbf{z}_{\mathbf{ij}})\end{aligned} \tag{A.15}$$

and

$$\mathbf{u}^{\mathrm{T}}K\mathbf{u} = \sum_{i\in\mathcal{B},j\in\mathcal{B}}\mathbf{u}_iK_{ij}\mathbf{u}_j + \sum_{i\in\mathcal{B},j\in\mathcal{D}}\mathbf{u}_iK_{ij}\mathbf{u}_j + \sum_{i\in\mathcal{D},j\in\mathcal{B}}\mathbf{u}_iK_{ij}\mathbf{u}_j. \tag{A.16}$$

This shows that the entries of the matrix $K$ consist of the force constants.

## References

[1] S.A. Adelman, J.D. Doll, Generalized Langevin equation approach for atom/solid-surface scattering: collinear atom/harmonic chain model, J. Chem. Phys. 61 (1974) 4242.
[2] S.A. Adelman, J.D. Doll, Generalized Langevin equation approach for atom/solid-surface scattering: general formulation for classical scattering off harmonic solids, J. Chem. Phys. 64 (1976) 2375.
[3] H.C. Andersen, Molecular dynamics simulations at constant pressure and/or temperature, J. Chem. Phys. 72 (1980) 2384–2393.
[4] N.W. Ashcroft, N.D. Mermin, Solid State Physics, Brooks Cole, 1976.
[5] B.J. Berne, R. Pecora, Dynamic Light Scattering: With Applications to Chemistry, Biology, and Physics, Dover Publication, 2000.

[6] W. Cai, M. de Koning, V.V. Bulatov, S. Yip, Minimizing boundary reflections in coupled-domain simulations, Phys. Rev. Lett. 85 (2000) 3213.
[7] K.S. Cheung, S. Yip, A molecular-dynamics simulation of crack-tip extension: the brittle-to-ductile transition, Model. Simul. Mater. Sci. Eng. 2 (1994) 865–892.
[8] A.J. Chorin, O.H. Hald, R. Kupferman, Optimal prediction and the Mori–Zwanzig representation of irreversible processes, Proc. Natl. Acad. Sci. USA 97 (2000) 6253–6257.
[9] A.J. Chorin, O.H. Hald, R. Kupferman, Optimal prediction with memory, Physica D 166 (2002) 239–257.
[10] A.J. Chorin, A. Kast, R. Kupferman, Optimal prediction of underresolved dynamics, Proc. Natl. Acad. Sci. USA 96 (1998) 4094–4098.
[11] A.J. Chorin, P. Stinis, Problem reduction, renormalization, and memory, Commun. Appl. Math. Comp. Sci. 1 (2005) 1–27.
[12] M.S. Daw, M.I. Baskes, Embedded-atom method: derivation and application to impurities, surfaces, and other defects in metals, Phys. Rev. B 29 (1984) 6443.
[13] W. E, Z. Huang, Matching conditions in atomistic-continuum modeling of material, Phys. Rev. Lett. 87 (2001) 135501.
[14] W. E, Z. Huang, A dynamic atomistic-continuum method for the simulation of crystalline material, J. Comput. Phys. 182 (2002) 234–261.
[15] W. E, P. Ming, Cauchy–Born rule and the stability of the crystalline solids: dynamic problems, Acta Math. Appl. Sin. Engl. Ser. 23 (2007) 529–550.
[16] J.L. Ericksen, The Cauchy–Born hypothesis for crystals, in: M. Gurtin (Ed.), Phase Transformations and Material Instabilities in Solids, 1984.
[17] D. Frenkel, B. Smit, Understanding Molecular Simulation: From Algorithms to Applications, second ed., Academic Press, 2002.
[18] S.P.A. Gill, Z. Jia, B. Leimkuhler, A.C.F. Cocks, Rapid thermal equilibration in coarse-grained molecular dynamics, Phys. Rev. B 73 (2006) 184304.
[19] B.L. Holian, R. Ravelo, Fracture simulation using large-scale molecular dynamics, Phys. Rev. B 51 (1995) 11275.
[20] D. Holland, M. Mardar, Cracks and atoms, Adv. Mater. 11 (1999) 793–806.
[21] W.G. Hoover, Constant-pressure equations of motion, Phys. Rev. A 34 (1986) 2499–2500.
[22] E.G. Karpov, H.S. Park, W.K. Liu, A phonon heat bath approach for the atomistic and multiscale simulation of solids, Int. J. Numer. Methods Eng. 70 (2007) 351–378.
[23] E.G. Karpov, G.J. Wagner, W.K. Liu, A Green's function approach to deriving non-reflecting boundary conditions in molecular dynamics simulations, Int. J. Numer. Methods Eng. 62 (9) (2005) 1250–1262.
[24] R. Kubo, The fluctuation–dissipation theorem, Reports Progress Phys. 29 (1) (1966) 255–284.
[25] X. Li, Stability of the Boundary Conditions for Molecular Dynamics, preprint submitted.
[26] X. Li, W. E, Variational boundary conditions for molecular dynamics simulations of solids at low temperature, Commum. Comput. Phys. 1 (2006) 136–176.
[27] X. Li, W. E, Boundary conditions for molecular dynamics simulations at finite temperature: treatment of the heat bath, Phys. Rev. B 76 (2007) 104107.
[28] A. Machova, G.J. Ackland, Dynamic overshoot in $\alpha$-iron by atomistic simulations, Model. Simul. Mater. Sci. Eng. 6 (1998) 521–542.
[29] G. Martyna, M. Tuckerman, D. Tobias, M. Klein, Explicit reversible integration algorithms for extended systems, Molecul. Phys. 87 (1996) 1117.
[30] S. Melchionna, G. Ciccotti, B.L. Holian, Hoover NPT dynamics for systems varying in shape and size, Molecul. Phys. 78 (1993) 533–544.
[31] R. Miller, E.B. Tadmor, R. Phillips, M. Ortiz, Quasicontinuum simulation of fracture at the atomic scale, Model. Simul. Mater. Sci. Eng. 6 (1998) 607–638.
[32] H. Mori, Transport, collective motion, and Brownian motion, Prog. Theor. Phys. 33 (1965) 423–450.
[33] A. Needleman, Numerical modeling of crack growth under dynamic loading conditions, Comput. Mech. 19 (1997) 463–469.
[34] M. Parrinello, A. Rahman, Polymorphic transition in single crystals: A new molecular dynamics method, J. Appl. Phys. 52 (1981) 7182.
[35] V. Shastry, D. Farkas, Molecular statics simulation of crack propagation in alpha-Fe using EAM potentials, in: Materials Research Society Symposium Proceedings, Boston, MA, United States, November 27–December 1, 1995, 1996, pp. 75–80.
[36] G.C. Sih, H. Liebowitz, Fracture, An Advanced Treatise, Academic Press, 1968.
[37] A. Stroh, Dislocations and cracks in anisotropic elasticity, Philos. Mag. 7 (1958) 625–646.
[38] E.B. Tadmor, M. Ortiz, R. Phillips, Quasicontinuum analysis of defects in crystals, Phil. Mag. A 73 (1996) 1529–1563.
[39] A.C. To, S. Li, Perfectly matched multiscale simulations, Phys. Rev. B 72 (2005) 035414.
[40] G.J. Wagner, E.G. Karpov, W.K. Liu, Molecular dynamics boundary conditions for regular crystal lattice, Comput. Method Appl. Mech. Eng. 193 (2004) 1579–1601.
[41] J.Z. Yang, X. Li, Boundary conditions for molecular dynamics simulations of solids: a comparative study, Phys. Rev. B 73 (2006) 224111.
[42] R. Zwanzig, Collision of a gas atom with a cold surface, J. Chem. Phys. 32 (1960) 1173.
[43] R. Zwanzig, Problems in nonlinear transport theory, in: L. Garrido (Ed.), Systems Far From Equilibrium, Interscience, New York, 1980.
[44] R. Zwanzig, Nonequilibrium Statistical Mechanics, Oxford University Press, 2001.